Effect of Facing Slope on the Seismic Response of Geocell Walls

Madhavi Latha G[1*] and Manju G. S.[1]
[1]*Department of Civil Engineering, Indian Institute of Science, Bangalore-560012, India*
E-mail: madhavi@civil.iisc.ernet.in

ABSTRACT: This paper presents the effect of slope angle of facing on the seismic response of retaining walls with geocell facing. Keeping the dimensions and configuration of geocell layer same, shaking table model tests were carried out with vertical and battered walls retaining sand backfill. In case of battered walls, geocell layers were laid with an offset, resulting in an overall slope of the wall. Vertical walls were constructed with geocell layers stacked vertically above each other. Gravel was used as infill material in geocells. Models were subjected to different levels of ground motion conditions by controlling the acceleration and frequency of shaking. Acceleration amplitudes of 0.2g and 0.3g with frequencies ranging between 1 Hz and 7 Hz were used in the model tests. Response of models was monitored with cyclic shaking at intended acceleration and frequency by measuring the face deformations and acceleration amplifications along the height of the retaining wall, Results from model tests showed that battered walls perform better than the vertical walls since the measured deformations and acceleration amplifications were comparatively low in battered walls. The improved performance of battered walls is due to the increased stiffness and increase in dynamic impedance caused due to shifting of moment of inertia of pressure distribution at the back of the wall in case of walls battered towards the backfill.

KEYWORDS: Geocells, Retaining walls, Seismic performance, RMSA amplification factor, Wall slope, Shaking table model studies

1. INTRODUCTION

Geocell is a three-dimensional, polymeric, honeycomb like cellular material. A network of these cells made to specific dimensions is used as 3-Dimenional form of geosynthetic reinforcement in soils. The specific benefits of geocells over conventional reinforcing geosynthetics like geotextile and geogrid is that geocell provides all-round confinement to the soil, which helps in reducing lateral deformations and spreads the imposed loads to wider areas, making them an attractive choice for foundations, retaining walls and embankments. The original concept of cellular confinement was developed by US Army Corps of Engineers (Rea and Mitchell 1978). The primary application was surface stabilization of granular soils under vehicular loading and military bridge approach roads over soft ground. (Webster and Watkins 1977; Martin and Senf 1995). Geocells were widely used during the Vietnam War and also during the Gulf operations in the late 1980s. Geocells are now manufactured by ultrasonically welding polymeric sheets. They can also be stitched using planar geotextiles or assembled at the site using geogrids. These geocells form a honey-comb like structure which can be filled with sand or gravel and compacted to form a rigid structure. Geocells have found a wide range of applications, including retaining wall construction, embankment base reinforcement, foundation support, subgrade stabilization, erosion control and slope protection, channel protection, flood protection or military protection barriers.

Planar geosynthetics like geotextiles and geogrids interact with the soil through surface friction and interlocking with soil particles. They prevent the lateral flow of soil only through these two mechanisms. Hence, these forms of reinforcement cannot be applied when lateral flow tendency is severe such as under heavy loads or in flowing water conditions. For such applications, three dimensional confinement of soils along with friction and interlocking (Figure 1), as provided by geocells is preferred.

Geocells facilitate the construction of steep vertical mechanically stabilized earth retaining structures. Stacking of geocell layers to create retaining walls and slopes has solved several issues like space constraints and complicated designs by allowing flexible design patterns with multifold increase in the load carrying capacity of these structures. Geocell walls are extremely flexible and hence the deformations are independent in each layer to an extent, thus avoiding cumulative deformations piled up at the top of the wall as seen in case of rigid retaining walls. Few specific advantages of geocell retaining walls (Racana et al. 2001; Chen and Chiu 2008; Chen et al. 2013) are listed below:

- Geocell retaining walls are structurally stable under self-weight and externally imposed loads, while the flexibility of the structure offers very high seismic resistance.
- Since geocell facing is wide and adds enormous stability to the wall unlike conventional Geosynthetic Reinforced Soil Walls (GRSW) or Mechanically Stabilized Earth Walls (MSEW), steeper and taller retaining walls are possible.
- Efficient drainage and storm water management is possible in geocell retaining walls. The outer fascia cells of the wall can be planted with vegetation to create a green wall.
- Use of low grade/local granular infill such as concrete waste can make geocell wall a cost effective solution when compared to other techniques.
- High stiffness and low creep of geocell materials make them attractive for sustained static and cyclic loading conditions.
- Geocells are highly resistant to temperature variations and chemical reactions and can be used in all types of soil conditions.

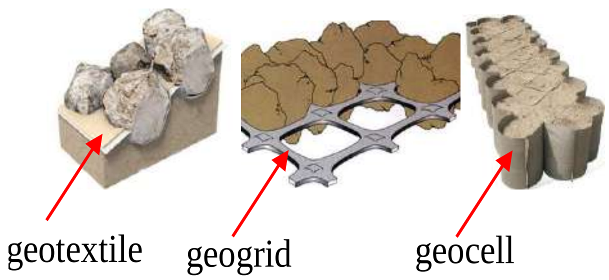

Figure 1 Mechanisms of interaction of different types of geosynthetics with soil/aggregate (compiled from google images)

Under static loading conditions, role of tensile reinforcement in retaining walls is to provide additional confinement to the soil, which can be realized as apparent cohesion, providing additional stability against sliding and overturning. During earthquake, the soil element under constant overburden pressure is subjected to cyclic simple shear stresses with alternating positive and negative values in addition to the vertical and horizontal normal stresses. These earthquake induced shear stresses increase the difference in principal stresses, thus enlarging the Mohr circle to bring the soil element close to a failure state (Ling et al. 2009). If the induced shear stresses are very high, the minor principal stress can be negative, thus inducing tension in soil. Since retaining walls are usually built with granular soils, which cannot sustain any tension, ground surface cracks develop. Cyclic rotation of principal stress directions also occurs under seismic loading conditions, which can significantly reduce the shear strength of soils, causing further instabilities. The tensile reinforcement offers restraint to the shear deformations in soil induced by seismic events. Compared to planar geosynthetic materials, geocells offer higher restraint to the shear deformations in the soil due to their higher stiffness and strength. Also, the locking effect of geocells, which ensures the soil to be confined within the pockets, further provides better resistance to shear deformations, making them more suitable for retaining walls which can be subjected to seismic ground shaking conditions.

The first geocell retaining wall was constructed in North America in 1988 (Bathurst and Crowe 1992). Many other walls were constructed since early 90's and the construction methodology for these walls is well established by now. Though the studies on retaining walls reinforced with geosynthetics are numerous, literature on geocell retaining walls is limited (Leschinsky et al. 2009; Ling et al. 2009). Very few studies are available on the seismic response of geocell retaining walls. Since geocell walls substantially differ with retaining walls reinforced with planar geosynthetics in their mechanism of interaction with soil and strain restraint effects, these aspects and their variation under the influence of various ground motion parameters and geometries need careful consideration and evaluation. This study is motivated by this need.

2. MATERIALS AND METHODS

Materials used in the study are fine sand as backfill material, gravel as geocell infill and geonets for making geocells. Properties of these materials are presented in following subsections.

2.1 Fine sand

Commercially available artificial fine sand which was obtained by crushing of rock was used for the study. The grain size distribution of this sand, determined by dry sieving is presented in Figure 2. This sand is classified as poorly graded sand designated as SP as per the Unified Soil Classification System. The index and gradation properties of this fine sand are reported in Table 1.

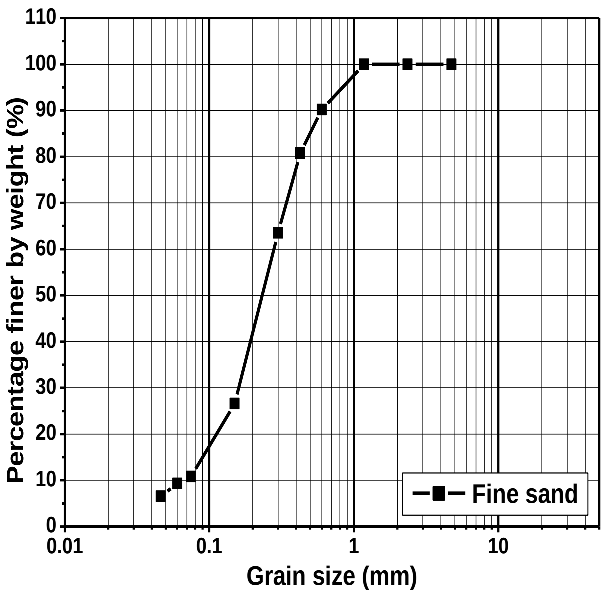

Figure 2 Grain size distribution of fine sand

Table 1 Properties of fine sand

Property	Value
Specific gravity	2.65
Effective opening size (D_{10})(mm)	0.065
Mean particle size D_{50} (mm)	0.3
Percentage fines (< 0.075mm) (%)	10
Co-efficient of Uniformity (C_u)	4.46
Co-efficient of Curvature (C_c)	1.36
Soil Classification	SP
Minimum unit weight (kN/m^3)	14.57
Maximum unit weight (kN/m^3)	17.91

2.2 Gravel

Gravel used in the study was poorly graded with an average size of 12 mm. Grain size distribution of gravel is given in Figure 3. Properties of gravel are given in Table 2.

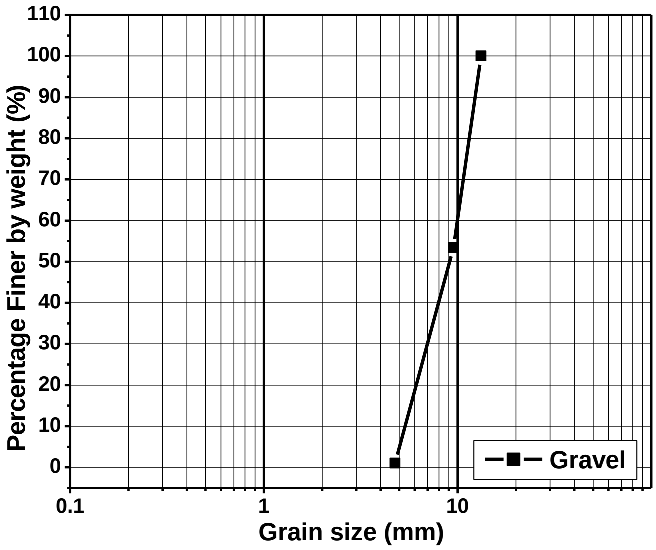

Figure 3 Grain size distribution of gravel

Table 2 Properties of gravel

Property	Value
Effective size (D_{10})(mm)	5.5
Co-efficient of Uniformity (C_u)	1.82
Co-efficient of curvature (C_c)	0.89
Mean particle size D_{50} (mm)	12
Soil classification	GP
Minimum unit weight (kN/m^3)	18.4
Maximum unit weight (kN/m^3)	21.5

2.3 Geonet

Geonet used in this study is made of High Density Polyethylene (HDPE) material, referred to as G2 in this paper. The load-deformation response of geonet obtained from standard multi-rib tension test (as per ASTM D 6637-01) is shown in Figure 4. Physical and tensile properties of geonet are given in Table 3. Geocells using G2 were made by connecting two geonet surfaces arranged in a honeycomb configuration, using a steel wire, manually run through the openings and tied at the end. Seam strength of geocells obtained from multi-rib tension test, with a seam at the mid-length of the sample is also shown in Figure 4.

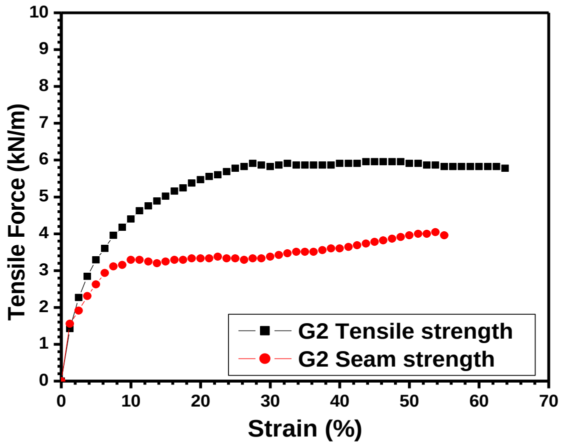

Figure 4 Load-elongation response of geonet

Table 3 Properties of geonet used for making geocells

Property	Value
Aperture size (mm × mm)	7×8
Aperture shape	Diamond
Thickness (mm)	3
Mass/unit area (g/m^2)	750
Ultimate tensile strength (kN/m)	5.96
Yield point strain (%)	49
Secant modulus at 1% strain (kN/m)	100
Seam Strength(kN/m)	4

3. SHAKING TABLE MODEL TESTS

3.1 Shaking Table Facility

A computer controlled servo hydraulic single degree of freedom (horizontal) shaking table facility was used in this study for simulating the horizontal shaking action, associated with seismic vibrations. Shaking table was connected to the digitally controlled servo-hydraulic actuator, which produces a horizontal seismic motion. The shaking table has a loading platform of 1 m × 1 m size with a payload capacity of 1 ton. The shaking table can be operated within the acceleration range of 0.05g to 2g and frequency range of 1 Hz to 50 Hz. The maximum stroke (displacement) value that can be achieved by the actuator is ±200 mm with a maximum force of 30 kN. Shaking table was manufactured to a natural frequency of 100 Hz to avoid resonance during tests. The major components of the shaking table are loading platform, loading frame, servo-hydraulic actuator and hydraulic power pack, digital controller and the application software. Problems with using rigid box containers for model preparation in a shaking table are: Reflection and generation of P-waves at the container boundary, side friction between soil and model container, which makes the measurements near the boundaries inaccurate and high lateral resistance offered by the box, which offers resistance to the deformation of soil. Hence researchers commonly use laminar boxes for shaking table testing to overcome these problems. A laminar box is a large shear box consisting of several frictionless horizontal layers. The layers move relative to one another in accordance with the deformation of the soil inside. Reflection or generation of P-waves is minimized and shear beam conditions are simulated in soil during vertical shear wave propagation. It has reduced side friction and minimized boundary effects, providing least resistance to the deformations of soil. The laminar box used for the tests is rectangular in cross section with inner dimensions of 1000 mm × 500 mm × 800 mm (Length × Width × Depth) with fifteen rectangular hollow aluminum layers. These layers are separated by linear roller bearings arranged to permit relative movement between the layers with minimum friction. Basic details of the shaking table system used in this study were given by Krishna (2008). Details of the new digital controller to monitor the table motion, its operation and application software (MTL-32) used to readout the response were given by Varghese (2014).

3.2 Model Construction

Models of geocell retaining walls were constructed inside the laminar box placed on the shaking table and instrumented with various sensors to monitor the response of the model walls during dynamic shaking. These sensors include accelerometers and non-contact ultrasonic displacement transducers (USDT). These sensors are connected to the junction box where the signals received from the sensors are amplified and then transmitted to the transducer mother board boxes and the digital controller. All these instruments are of analog voltage output type and generate continuous data to the application software as the test progresses. The basic application software MTL-32 includes user interface required for setting up the test system including calibration, data acquisition, servo tuning, limit interlocks and manual programming.

Accelerations are measured using accelerometers which are of analog voltage output type with a full-scale acceleration range of ± 2g within the bandwidth of 1 Hz - 2 kHz. The accelerometers are sensitive to measure the accelerations in the order of 0.001g. Non-contact type ultrasonic displacement transducers were used to measure the facing displacements of the retaining wall. These sensors emit one or multiple pulses of ultrasonic energy, which travel through the air at the speed of sound. A portion of this energy reflects off the target and travels back to the sensor. The sensor measures the total time required for the energy to reach the target and return to the sensor and calculates the displacement of the target from the changing distance of the target from the sensor. The sensing range of these sensors is 30 mm to 300 mm with short dead zone of 30 mm and output response time of 30 ms.

Shaking table tests were conducted to study the performance of the geocell retaining walls under seismic conditions. Studies were conducted varying the ground motion parameters and retaining wall configuration. Under ground motion parameters, acceleration and frequency of base shaking were varied. Retaining walls with vertical and battered slopes were tested in different model tests. All model retaining walls had a base dimensions of 800 mm × 500 mm. The plan dimensions of the top of the retaining wall was 550 mm × 500 mm for battered retaining walls and 800 mm × 500 mm for vertical walls. Height of the retaining wall was kept constant as 600 mm. Initially, a polyethylene sheet was tightly fixed to the inner sides of the laminar box using an adhesive tape to cover the gap between the rectangular panels of the laminar box and also to minimize the friction between the model and laminar box. The walls were constructed in 6 layers, each layer being 100 mm high, which is equal to the height of the geocell layers. Geocell layers with pocket size of 100 mm and height 100 mm were prepared on a basal geogrid of same material, to maintain the dimensions of cells.

To start with, the dimensions of the retaining wall and the position of bottom most geocell layer were marked on the laminar box. The first geocell layer fixed to the basal geosynthetic layer was positioned at the base of the laminar box in the marked area at the wall facing. The geocell wall section was overfilled with the specified infill material and levelled to approximately 5 mm above the cell wall. The infill material was then compacted using a compaction rod to a relative density if 70%. Extra fill material above the top level of geocell layer was then carefully removed using a steel scale, making sure that the geocells and the infill are in flush with each other. The geocell installation procedures for retaining walls outlined by US Fabrics Inc. (2009) were carefully followed while installing the geocell layers. The quantity of backfill sand required for the first layer of the retaining wall was calculated and poured behind the geocell facing and compacted. Care was taken that each layer of sand was compacted thoroughly so that it is in flush with the geocells of that particular layer. Relative density of backfill was kept as 70% in all tests. The next layer of geocell was laid directly above the first layer at the facing in case of vertical walls and the compaction procedure is continued. In case of battered walls, an offset of 50 mm from the previous layer was maintained, resulting in an overall batter of 67.4°. Schematic diagrams of the battered wall and vertical walls are given in Figure 5. Photographs of battered and vertical walls are shown in Figure 6.

(a) (b)

Figure 6 Photographs of the model retaining walls
(a) battered wall (b) vertical wall

During the process of compaction of geocell fill material, accelerometers, A1, A2 and A3 were embedded in the geocell at elevations 150 mm, 350 mm and 550 mm, respectively from the base of the wall. The accelerometer, A0 fixed to the base of the shaking table measures the base acceleration. In some tests, the accelerometers were embedded in the backfill also to compare the acceleration response of the backfill and the facing. Three displacement transducers, D1, D2 and D3, were positioned along the facing of the wall at elevations 150 mm, 350 mm and 550 mm, respectively from the base of the wall to measure the horizontal displacements. USDTs were positioned in place using a T-shaped bracket made up of standard L-section that is rigidly connected to the laminar box frame and base. These USDTs are of shock proof type, which can give accurate measurements at accelerations up to of 10g and frequencies up to 60 Hz.

3.3 Similitude Laws

For the model geocell retaining walls tested in the present study, the size of the model is determined based on the dimensions of the shaking table facility available. The stress levels in the experiments do not truly represent the stresses in field because of the gravity effects and boundary effects in model studies. In order to make use of the results obtained from model tests to the respective full size prototype, scaling laws are used. Iai (1989) presented similitude laws for the 1 g model tests from basic definitions of effective stress, strain and constitutive law, overall equilibrium and mass balance. A geometric scale factor, λ_M was defined as the proportionality constant between the model and prototype geometry. These similitude laws were later verified by several researchers for studies related to seismic behaviour of soil structures (Lin and Wang, 2006; Mirlatifi et al., 2007; Chen and Chiu, 2008; Guler and Enunlu, 2009). For the present study, the geometric scale factor, λ_M, is taken as 10. Accordingly, the height of the model retaining wall was kept as 0.6 m, corresponding to 6 m in field. The scaling factors computed for various physical quantities in models to those in prototype are given in Table 4.

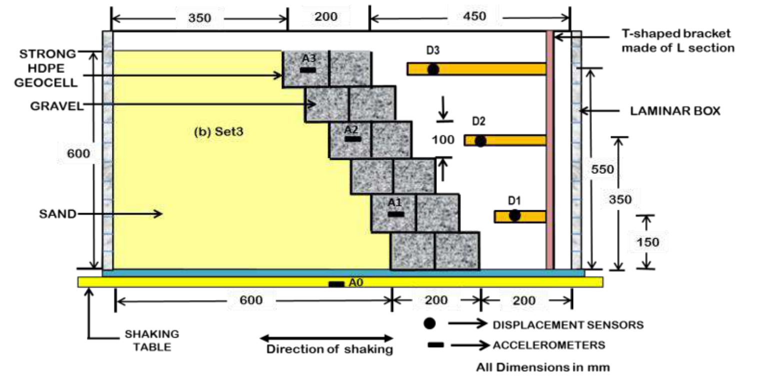

(a) Battered wall

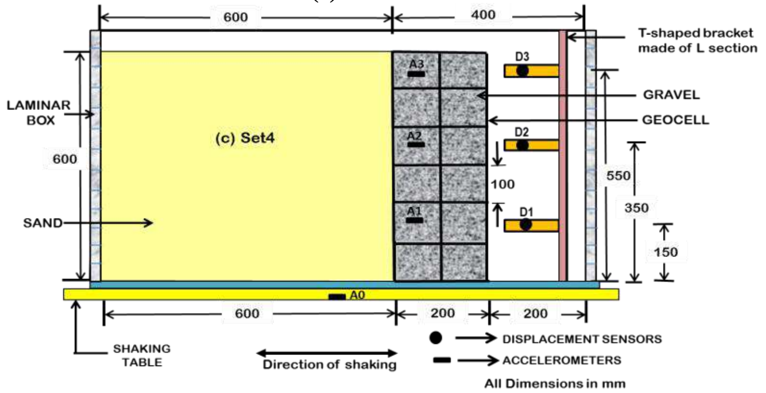

(b) Vertical wall

(c) Figure 5 Schematic diagrams of the model retaining walls

Table 4 Scaling factors based on similitude laws

Parameter	Model parameter	Equation for scaling factor	Scaling factor	Prototype parameter
Acceleration(g)	0.2, 0.3	1	1	0.2, 0.3
Height of the wall (m)	0.6	λ_M	10	6
Width of the wall *B* (m)	0.5	λ_M	10	5
Unit weight of Soil (kN/m^3)	17	1	1	17
Frequency (Hz)	f_m	$1/(\lambda_M)^{3/4}$	0.178	$0.178 \times f_m$
Stress	σ_m	λ_M	10	$10 \times \sigma_m$
Time	t_m	$\lambda_M{}^{3/4}$	5.62	$5.62 \times t_m$
Reinforcement stiffness	J_m	$\lambda_M{}^2$	10	$100 \times J_m$

3.3 Model Tests

All model walls were subjected to 100 cycles of horizontal base shaking, at intended acceleration and frequency. The vertical component of an earthquake record is not considered in this study as it is often much smaller than the horizontal acceleration component for most earthquakes, and rarely peaks at the same time as the horizontal ground acceleration (Seed and Whitman, 1970). Models were subjected to two different horizontal accelerations, 0.2g and 0.3g at frequencies ranging between 1Hz and 7Hz. Table 5 presents the test matrix used for the model tests on retaining walls with battered and vertical wall facing. The test code represents the test series, acceleration of shaking and frequency of shaking. Battered walls were represented by S3 and vertical walls were represented by S4 in this study. Test code S3A2F1 represents the test battered wall subjected to an acceleration of 0.2g and frequency of 1 Hz.

Table 5 Test matrix for shaking table model tests

Sl. No	Wall facing	Test code	Acceleration (g)	Frequency (Hz)
1	Battered	S3A2F1	0.2	1
2	Battered	S3A2F2	0.2	2
3	Battered	S3A2F3	0.2	3
4	Battered	S3A2F7	0.2	7
5	Battered	S3A3F1	0.3	1
6	Battered	S3A3F2	0.3	2
7	Battered	S3A3F3	0.3	3
8	Battered	S3A3F7	0.3	7
9	Vertical	S4A2F1	0.2	1
10	Vertical	S4A2F2	0.2	2
11	Vertical	S4A2F3	0.2	3
12	Vertical	S4A2F7	0.2	7
13	Vertical	S4A3F1	0.3	1
14	Vertical	S4A3F2	0.3	2
15	Vertical	S4A3F3	0.3	3
16	Vertical	S4A3F7	0.3	7

4. RESULTS AND DISCUSSION

Acceleration response from a typical model test measured from 4 different accelerometers A0, A1, A2 and A3 is presented in Figure 7. Base acceleration is 0.3g for this case, which is measured through A0 and the amplified responses at different elevations are measured through A1, A2 and A3 as shown in the figure. Similarly, displacement response from a typical model test is presented in Figure 8. Displacements measured at elevations 150 mm, 350 mm and 550 mm from the base were measured using displacement sensors D1, D2 and D3, respectively, as shown in the figure.

Displacements of wall facing measured in different model tests on battered and vertical walls at an acceleration amplitude of 0.2g are shown in Figure 9 for frequencies 1 Hz and 2 Hz and in Figure 8 for frequencies of 3 Hz and 7 Hz. Displacements for these walls at an acceleration amplitude of 0.3g are shown in Figure 9 for frequencies 1 Hz and 2 Hz and in Figure 10 for frequencies of 3 Hz and 7 Hz. The model retaining walls with vertical facing displaced more horizontally than the retaining walls with a battered facing. From Figures 9a, it is clear that the horizontal displacement at the top of the retaining wall for an acceleration amplitude of 0.2g and a frequency of 1 Hz is 4.2 mm for battered wall and 5 mm for vertical wall. A 22% increase in horizontal deformations is observed for vertical walls compared to battered walls. Similarly, Figure 7b shows that the horizontal displacement for 2 Hz is 4.8 mm for battered wall and 6.3 mm for vertical wall, indicating 31% more horizontal deformations in case of vertical walls. As observed from Figure 10a and Figure 10b, the increase in horizontal deformations in case of vertical walls is 49% and 62%, for frequencies 3 Hz and 7 Hz, respectively, at an acceleration amplitude of 0.2g.

Figure 11a shows that the horizontal displacement at the top of the retaining wall for an acceleration amplitude of 0.3g and a frequency of 1 Hz is 5 mm for the battered wall and 8 mm for the vertical wall, indicating a 62% increase in deformations for vertical walls. Fig. 11b shows that the deformation values for 2 Hz are 5.5 mm and 9.5, for battered and vertical walls respectively, indicating an increase of 73% in horizontal deformations for vertical walls. The increase in deformations in case of vertical walls is 69% for both 3 Hz and 7 Hz frequencies at an acceleration amplitude of 0.3g, as calculated from Figure 12. It is very clear that battered walls deformed much lesser compared to vertical walls, the improved performance more evident at higher seismic loads. Shifting of center of gravity of wall facing weight towards the backfill in case of battered walls helped in achieving improved base stability and overall wall stiffness.

Sadrekarimi (2015) compared the seismic performance of vertical gravity walls and broken rock walls with inward and outward batter through shaking table tests. The estimated horizontal thrust for walls leaning towards the backfill is much smaller than the thrust in case of vertical walls. The seismic acceleration considered for this study was 0.25g, which falls within the range of acceleration amplitudes considered in the present study. Also the computed overturning moments for walls battered towards the backfill are lesser compared to those in vertical walls because of the shifting of the centroid of pressure distribution on the back of the wall since the application point of lateral thrust drops lower. With increase in acceleration amplitude or increase in frequency of shaking, the reduction in lateral thrust and overturning moment become more significant due to increased backfill inertia. Hence battered walls performed much better under seismic loads compared to vertical walls, especially at higher frequencies and acceleration amplitudes.

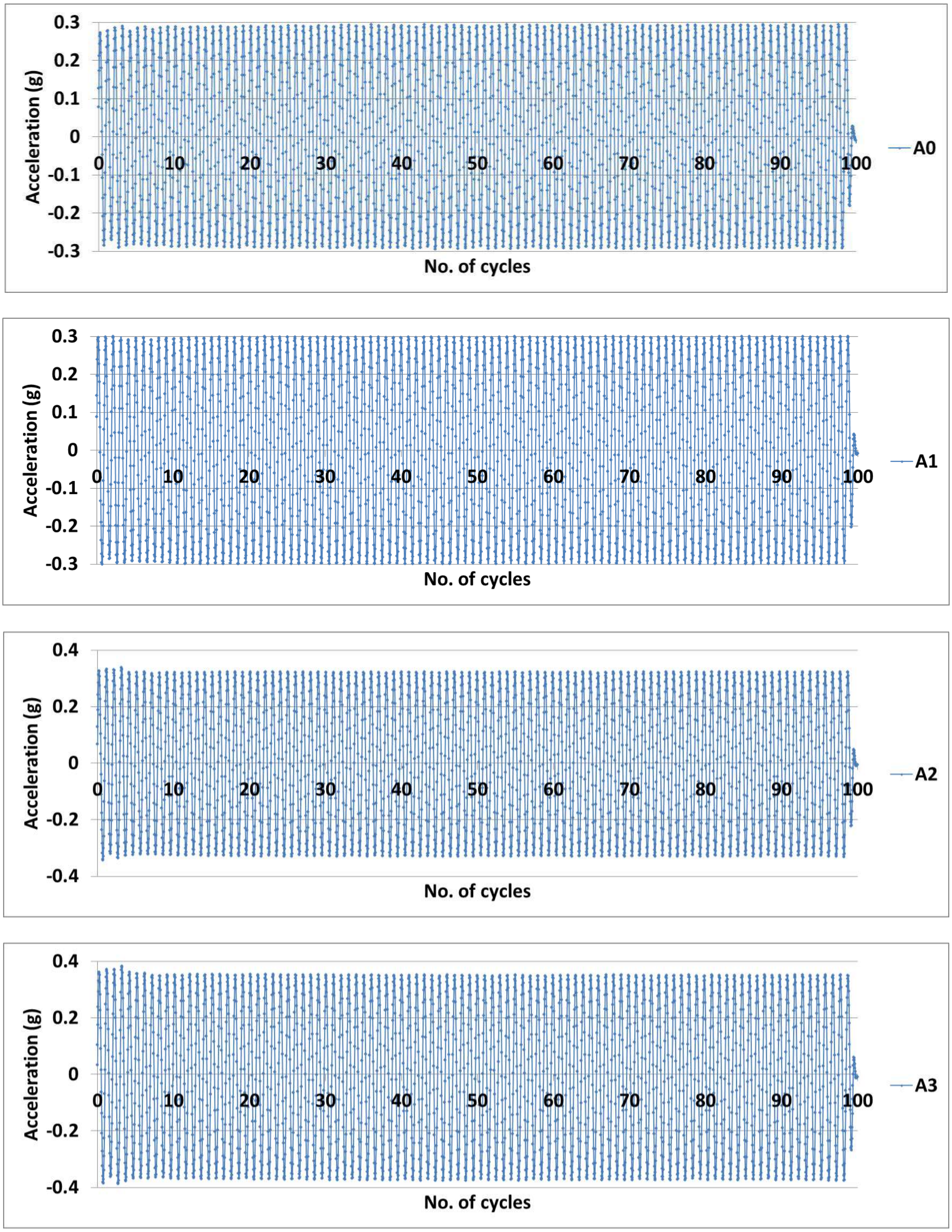

Figure 7 Typical acceleration response from a model test

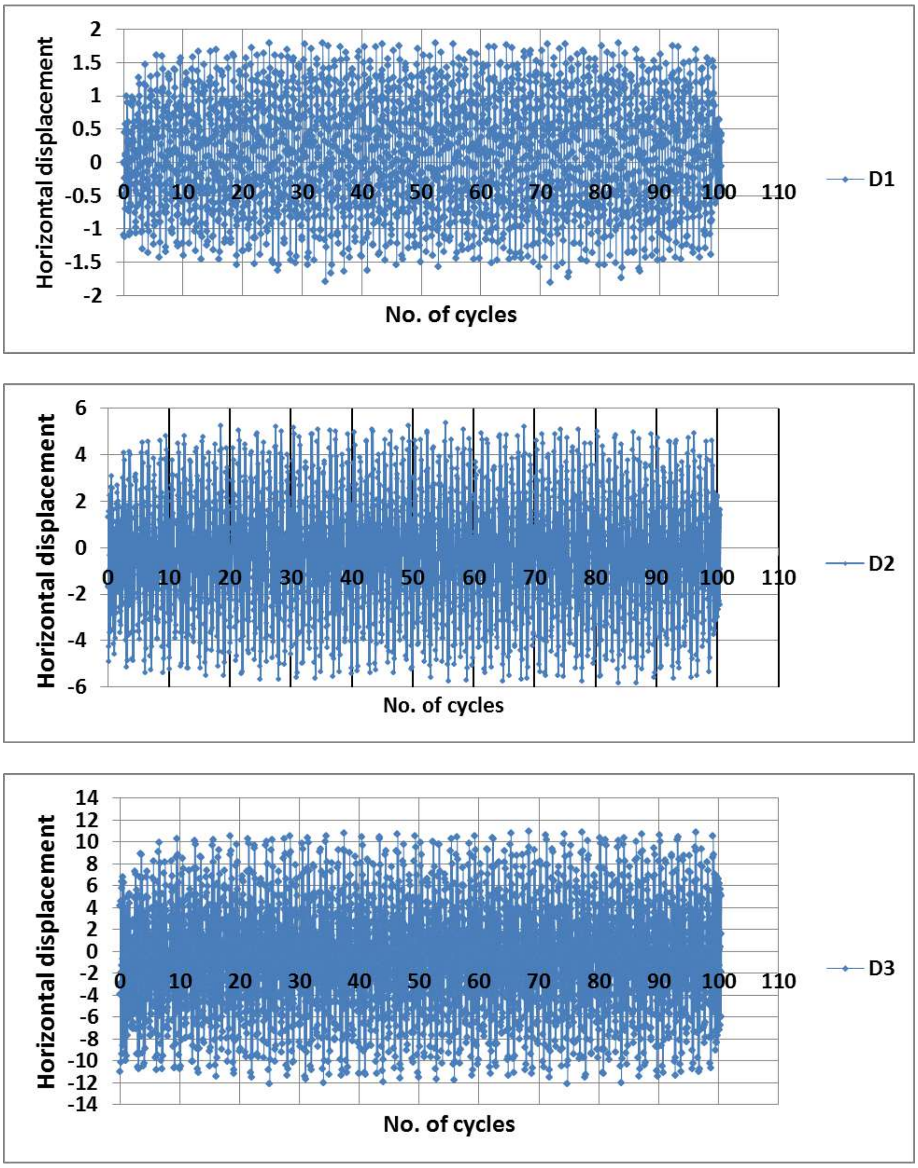

Figure 8 Typical displacement response from a model test

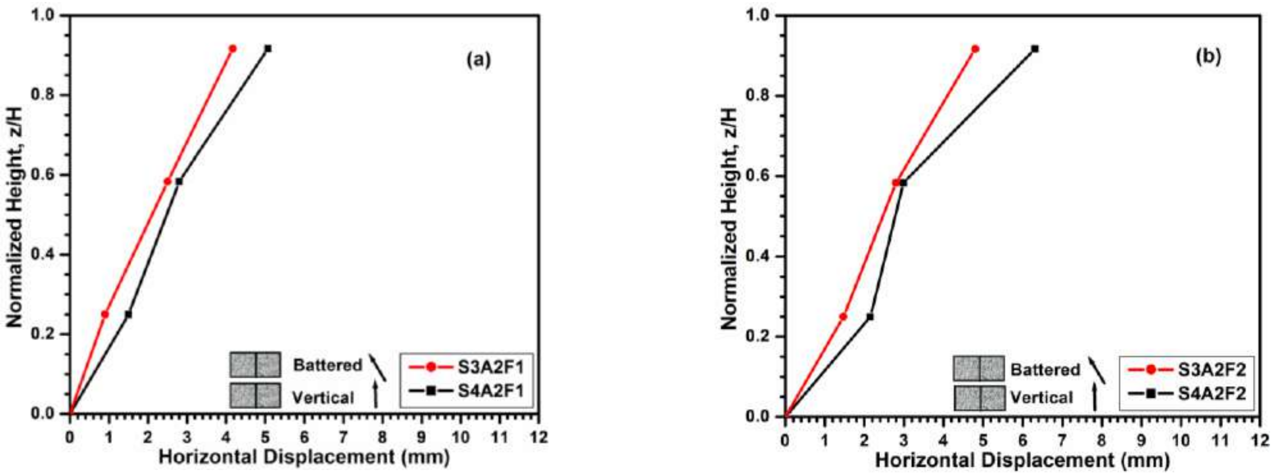

Figure 9 Variation of horizontal displacement of the wall facing for normalized height showing the effect of slope angle in geocell configuration for battered and vertical walls at 0.2g (a) 1Hz (b) 2 Hz

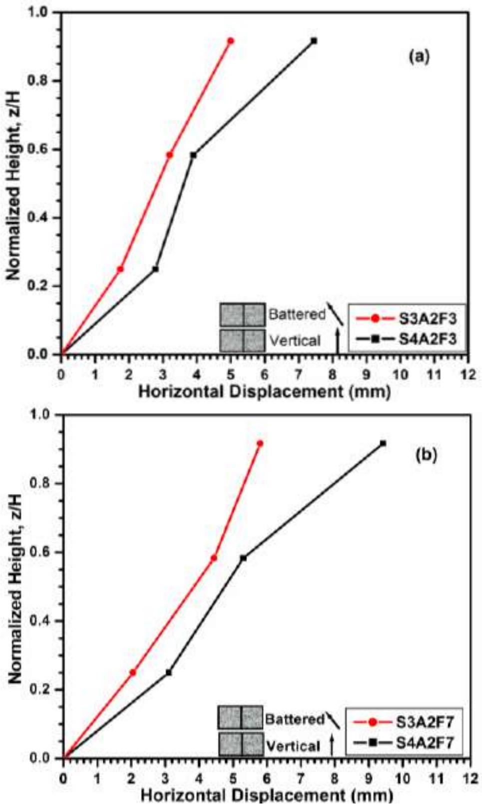

Figure 10 Variation of horizontal displacement of the wall facing for normalized height showing the effect of slope angle in geocell configuration for battered and vertical walls at 0.2g (a) 3Hz (b) 7 Hz

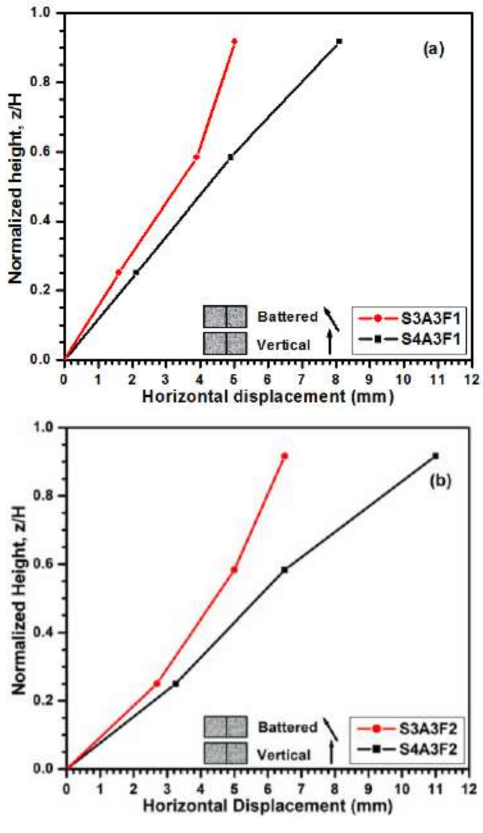

Figure 11 Variation of horizontal displacement of the wall facing for normalized height showing the effect of slope angle in geocell configuration for battered and vertical walls at 0.3g (a) 1Hz (b) 2 Hz

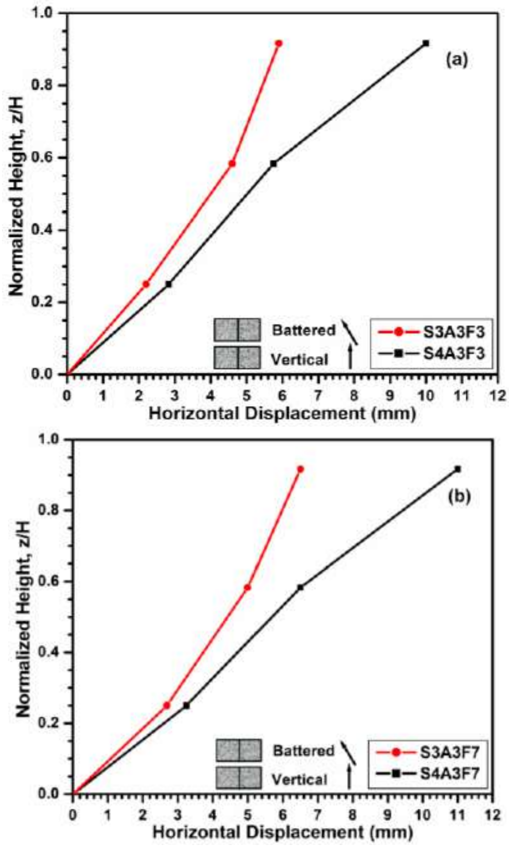

Figure 12 Variation of horizontal displacement of the wall facing for normalized height showing the effect of slope angle in geocell configuration for Set3 and Set4 for 0.3g (a) 3Hz (b) 7 Hz

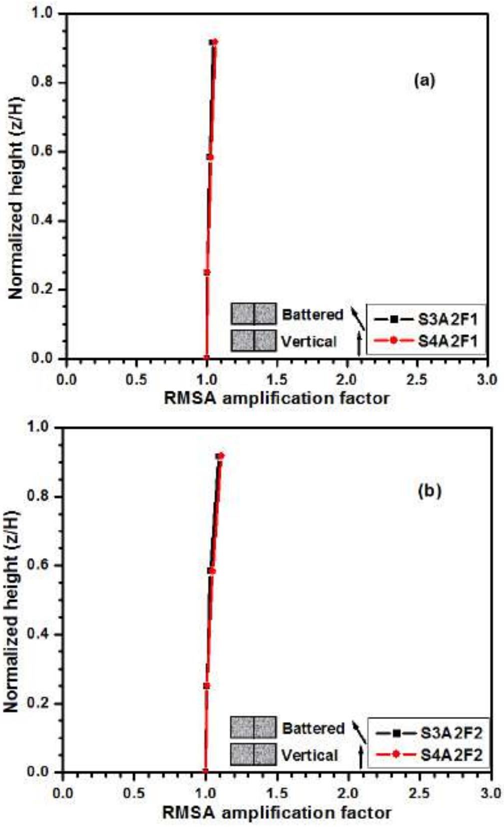

Figure 13 Variation of RMSA amplification factors with normalized height showing the effect of sloping angle in geocell configuration for battered and vertical walls for 0.2g (a) 1 Hz (b) 2 Hz

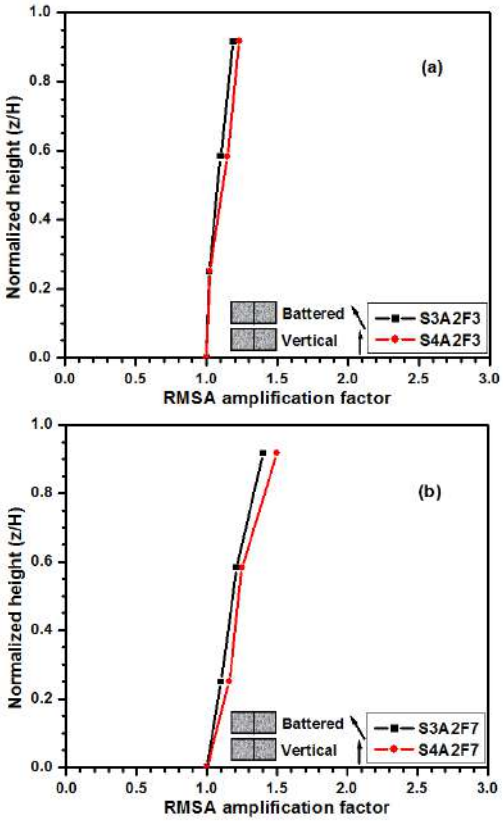

Figure 14 Variation of RMSA amplification factors with normalized height showing the effect of sloping angle in geocell configuration for battered and vertical walls for 0.2g (a) 3 Hz (b) 7 Hz

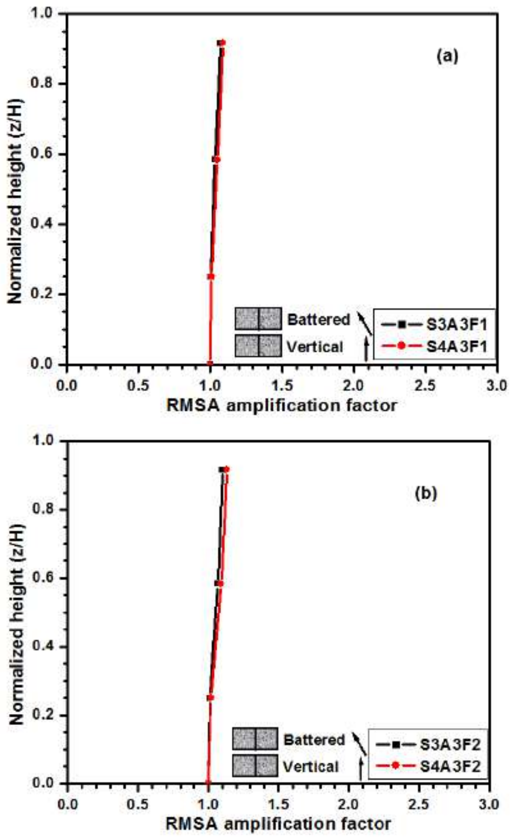

Figure 15 Variation of RMSA amplification factors with normalized height showing the effect of sloping angle in geocell configuration for battered and vertical walls for 0.3g (a) 1 Hz (b) 2 Hz

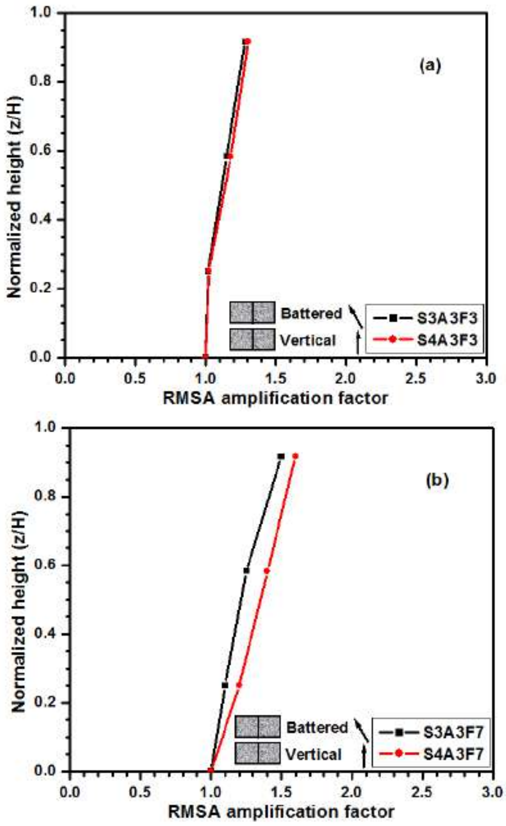

Figure 16 Variation of RMSA amplification factors with normalized height showing the effect of sloping angle in geocell configuration for battered and vertical walls for 0.3g (a) 3 Hz (b) 7 Hz

Further, amplification factors increase with the frequency of shaking as the frequency of shaking gets closer to the fundamental frequency of the retaining wall. Fundamental frequency of retaining wall models can be estimated approximately using the empirical formula proposed by Richardson (1978) and verified by Hatami and Bathurst (2000) for with retaining wall width to height ratio less than 3 with sandy backfills, given as

$$f_n = \frac{38.1}{H} \tag{1}$$

where f_n is the estimated fundamental frequency of the reinforced-soil wall in Hz and H is the wall height in meters. For the model walls in this study, the fundamental frequency calculated as per this empirical formula is about 63 Hz. Hatami and Bathurst (2000) suggested that Richardson's (1978) formula overestimates the fundamental frequency of retaining wall models. The range of frequencies used in the present study (1-7 Hz) are much lower than the estimated fundamental frequency. However, as the frequency of shaking increased, the amplification factors increased slightly, as the shaking frequency is getting closer to the fundamental frequency of the walls.

Crest settlements were measured in reinforced and unreinforced portions of the backfill at the end of the test at different points. Visual observations showed that since the cells were filled with gravel, in all the sets of tests, quite a bit of backfill sand was flowing into the rear cells because of large void spaces available, causing the formation of small craters at the end of geocell fascia. In case of Set4 configuration, this flow of fine sand into the rear cells was found to be the most, resulting in higher settlements at the junction of the backfill sand and gravel filled geocells. Measured crest settlements at the end of 100 cycles of shaking for both the vertical and battered wall configurations measured from the bottom most point of the wall facing are shown in Figure 17. Crest settlements were more than the horizontal deformations of the wall under seismic excitation. As the applied cyclic shear stress causes vibration and densification of the cohesionless fill materials, crest settles and the settlement is non-uniform since the backfill and geocell infill materials are different.

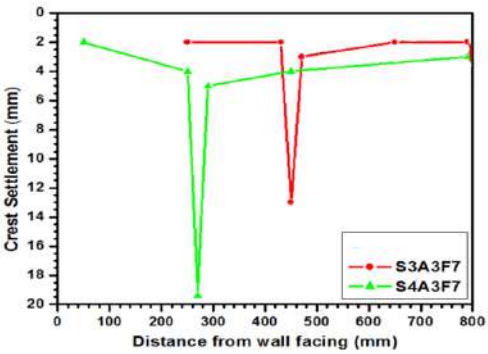

Figure 17 Variation of crest settlement with distance from the wall facing for battered and vertical walls at shaking of 0.3g and 7 Hz

Material cost in terms of backfill sand is often a key factor in determining the choice of a geocell retaining wall system, given the fast depletion of sand as a construction material. The vertical wall has a backfill volume of 0.18 m^3 and the battered wall has a backfill volume of about 0.13 m^3 (refer to Figure 5), about 27% lesser than the vertical wall in this study. The only advantage of having a vertical facing is the increased crest width available for movement of vehicles. If the crest space is not a criterion for designing the wall, lot of reduction in cost can be achieved by providing a bettered facing, in addition to the much improved stability against seismic loads. To attain the same stability levels as battered walls, the thickness of facing can be increased for vertical walls, which further increases the cost of these walls because of increased backfill volume, geocell infill volume and geocell area. Further, growing vegetation in geocell units is feasible in case of battered walls, which conceals the unevenness in facing geometry apart from improving the stability and also renders an aesthetic appearance to the facing.

Enough care is taken in the model tests presented in this study by repeating several tests to ensure the repeatability of model preparation and testing. Results obtained from the studies provide realistic insights into the behavior of geocell retaining walls in terms of deformations and acceleration amplifications. However, the major limitation of the study is that the experiments could not be validated with field data because no instrumented study on seismic response of geocell walls is available in literature. Further, the study is limited to horizontal shaking alone and in case of very strong seismic events where vertical component of shaking also plays significant role on the performance of walls, results from this study fall short of providing accurate predictions of deformations and acceleration amplifications, though the comparative study on vertical and battered walls is still valid for all cases and the relative wall performances remain the same. Though scaling laws applied in this study are valid and verified by several researchers and the use of laminar box greatly reduces the boundary effects, direct extrapolation of the results to field scale problems needs further evaluation and validation.

5. CONCLUSIONS

Shaking table model tests carried out on geocell retaining walls at different frequencies and accelerations showed that the walls undergo higher deformations and acceleration amplifications at higher frequencies and amplitudes of shaking. Results from model tests on vertical and battered walls showed that battered walls perform better than the vertical walls. The measured deformations and acceleration amplifications were comparatively low in battered walls. The improved performance of battered walls is due to the increased stiffness and increase in dynamic impedance caused due to shifting of moment of inertia of pressure distribution at the back of the wall, which helped in achieving improved base stability in case of battered walls. The difference in performance of these two types of walls is more evident at higher frequencies and acceleration amplitudes. If larger crest area is not a criterion for designing the wall, lot of reduction in cost can be achieved by providing a bettered facing to geocell walls, in addition to the much improved stability against seismic loads.

6. REFERENCES

ASTM D 6637-01 Standard Test Method for Determining Tensile Properties of Geogrids by the Single or Multi-Rib Tensile Method. ASTM International, PA, USA.

Bathurst, R. J. and Crowe, R.E. (1992) “Recent case histories of flexible geocell retaining walls in North America”, In Recent Case Histories of Permanent Geosynthetic-Reinforced Soil Retaining Walls, ed. F. Tatsuoka and D. Leshchinsky. A. A. Balkema, Rotterdam, pp. 3-20.

Chen, R. H. and Chiu, Y. M. (2008) “Model tests of geocell retaining structures”, Geotextiles and Geomembranes 26, Issue 1, pp. 56−70.

Chen, R. H., Huang, Y. W. and Huang, F. C., (2013) “Confinement effect of geocells on sand samples under triaxial compression”, Geotextiles and Geomembranes, 37, pp. 35-44.

Guler, E. and Enunlu, A.k. (2009) “Investigation of dynamic behavior of geosynthetic reinforced soil retaining structures under earthquake loads”, Bull. Earthquake Eng. 7, pp. 737–777.

Hatami, K. and Bathurst, R.J. (2000) “Effect of structural design on fundamental frequency of reinforced-soil retaining walls”, Soil Dynamics and Earthquake Engineering, 19, pp.137–157.

Iai, S. (1989) “Similitude for shaking table tests on soil-structure-fluid models in 1g gravitational field”, Soils and Foundations 29, pp. 105-118.

Kramer, S. L. (1996) Geotechnical Earthquake Engineering. Prentice Hall, Upper Saddle River, NJ, USA.

Krishna, A.M. (2008) Seismic response of geosynthetic reinforced soil wall models using shaking table tests, Ph.D. Thesis, Indian Institute of Science, Bangalore, India.

Krishna, A. M. and Latha, G. M. (2009) “Seismic behaviour of rigid-faced reinforced soil retaining wall models: reinforcement effect”, Geosynthetics International, 16(5), pp. 364 –373.

Leshchinsky, D., Ling, H. I., Wang, J.-P., Rosen, A., and Mohri, Y. (2009) “Equivalent seismic coefficient in geocell retention systems”, Geotextiles and Geomembranes, 27(1), pp. 9–18.

Lin, M.L. and Wang, K.L. (2006) “Seismic slope behavior in a large-scale shaking table model test Engineering”, Engineering Geology, 86, pp. 118–133.

Ling, H.I., Leshchinsky, D., Wang, J.P., Mohri, Y, and Rosen, A. (2009) “Seismic Response of Geocell Retaining Walls: Experimental Studies”, ASCE Journal of Geotechnical and Geoenvironmental Engineering, 135, Issue 4, pp. 515-524.

Martin, S., and Senf, D., (1995) "Cellular Confinement: An Important Technology for Soil Stabilization Applications", Geotechnical Fabrics Report, IFAI, January/February 1995, 13, Issue 1.

Mirlatifi, S.A., Fakher, A. and Ghalandarzadeh, A. (2007) “Seismic study of reinforced earth walls by shaking table model tests", 4th International Conference on Earthquake Geotechnical Engineering, Thessaloniki, Greece, Paper #1253.

Racana, N., Gourves, R. and Grediac, M. (2001) "Mechanical behaviour of soil reinforced with geocells", Journal of Geotechnical and Geoenvironmental Engineering, ASCE, 32(3), pp. 388–400

Rea, C., and Mitchell, J.K. (1978). "Sand reinforcement using paper grid cells", Preprint 3130, ASCE spring convention and exhibit, Pittsburgh, PA, pp. 644-663.

Richardson, G.N. (1978) "Earthquake resistant reinforced-earth walls", Proceedings of ASCE, Symposium on Earth Reinforcement, Pittsburgh, PA, pp. 664–684.

Sadrekarimi, A. (2015). "Gravity retaining walls: Reinvented." 6th International Conference on Earthquake Geotechnical Engineering, Christchurch, New Zealand, Paper #28.

Seed, H.B., and Whitman, R.V. (1970) "Design of earth retaining structures for dynamic loads". In Proceedings of the ASCE Special Conference on Lateral Stresses, Ground Displacement and Earth Retaining Structure, Ithaca, N.Y., pp. 103–147.

Truong, H.V.P. (2012) "Dynamic site-amplification factors and dynamic a attenuation factors by dynamic soil mass", Proceedings of 15th World Conference on. Earthquake Engineering, Lisbon, Portugal, pp. 1847-1856.

US Fabrics Inc. (2009) Geocell Installation Guideline: Retaining Walls, Guideline Document, US Fabrics Inc., Cincinnati, OH, USA.

Varghese, R.M. (2014) Shaking table tests to study the influence of ground motion, soil and site parameters on the initiation of liquefaction in sands, Ph.D. Thesis, Indian Institute of Science, Bangalore, India.

Webster, S. L., and Watkins, J. E. (1977). "Investigation of construction techniques for tactical bridge approach roads across soft ground" Tech Rpt. S-77-1, United States. Army. Corps of Engineers; Soils and Pavements Laboratory, USA.